A quantitative analysis of two-dimensional manually segmented transrectal ultrasound axial images in planning high dose rate brachytherapy for prostate cancer

Kvantitativna analiza aksijalnih dvodimenzionalnih ručno segmentisanih slika dobijenih primenom transrektalnog ultrazvuka u planiranju brahiterapije tumora prostate visokim brzinama doze

Kata Dabić-Stanković*[†], Katarina Rajković[‡], Miodrag Aćimović[†§],
Nebojša Milošević[‖], Jovan Stanković[†¶]

*Institute for Oncology and Radiology of Serbia, Belgrade, Serbia; [†]General Hospital
"Medical System Belgrade", Belgrade, Serbia; [‡]Institute of Biophysics, Faculty of Medicine,
University of Belgrade, Belgrade Serbia; [§]Clinic of Urology, Clinical Center of Serbia,
Belgrade, Serbia; [‖]Faculty of Medicine, University of Belgrade, Belgrade, Serbia;
[¶]High Medical School, Belgrade, Serbia

Abstract

Background/Aim. Prostate delineation, pre-planning and catheter implantation procedures, in high-dose rate brachytherapy (HDR-BT), are commonly based on the prostate manually segmented transrectal ultrasound (TRUS) images. The aim of this study was to quantitatively analyze the consistency of prostate capsule delineation, done by a single therapist, prior to each HDR-BT fraction and the changes in the shape of the prostate capsule during HDR-BT, using two dimensional (2D) TRUS axial image. **Methods.** A group of 16 patients were treated at the Medical System Belgrade Brachytherapy Department with definitive HDR-BT. The total applied median dose of 52 Gy was divided into four individual fractions, each fraction being delivered 2–3 weeks apart. Real time prostate axial visualization and the manual segmentation prior to each fraction were performed using B-K Medical ultrasound. Quantitative analyses, analysis of an area and shape were applied on 2D-TRUS axial images of the prostate. Area analyses were used to calculate the average value of the cross-sectional area of the prostate image. The parameters of the prostate shape, the fractal dimension and the circularity ratio of the prostate capsule contour were estimated at the maximum axial cross section of the prostate image. **Results.** The sample group consisted of four phases, each phase being performed prior to the first, second, third and fourth HDR-BT fraction, respectively. Statistical analysis showed that during HDR-BT fractions there were no significant differences in the average value of area, as well as in the maximum shape of prostate capsule. **Conclusions.** Quantitative analysis of TRUS axial prostate segmented images shows a successful capsule delineation in the series of manually segmented TRUS images, and the prostate maximum shape remaining unchanged during HDR-BT fractions.

Key words:
prostatic neoplasms; ultrasonography; brachytherapy; models, theoretical.

Apstrakt

Uvod/Cilj. Ocrtavanje kapsule prostate, preplaniranje i procedure primene katetera u brahiterapiji visokim brzinama doze [*high-dose rate brachytherapy* (HDR-BT)] zasniva se na ručnoj segmentaciji transrektalne ultrazvučne (TRUS) slike. Cilj rada bio je da se korišćenjem dvodimenzionalne TRUS aksijalne slike kvantitativno analizira konzistentnost ocrtavanja kapsule prostate za svaku HDR-BT frakciju, kao i promena oblika kapsule prostate tokom HDR-BT. **Metode.** Na grupi od 16 bolesnika bila je primenjena definisana HDR-BT u Odeljenju za brahiterapiju privatne opšte bolnice – Medicinski sistem Beograd. Ukupna primenjena srednja doza na metu od 52 Gy bila je podeljena u četiri individualne frakcije i svaka frakcija primenjena sa pauzom od dve do tri nedelje. Aksijalna vizualizacija prostate i ručno segmentisanje pre svake fracije izvedeno je pomoću ultrazvučnog uređaja B-K Medical. Ocrtavanje je vršio isti terapeut. Kvantitativna analiza, analiza površine i oblika prostate bila je primenjena na 2D-TRUS aksijalne slike prostate za svakog bolesnika posebno. Analiza površine koristila se za izračunavanje srednje vrednosti površine poprečnog preseka prostate. Parametri oblika prostate, fraktalna dimenzija i cirkularnost konture kapsule prostate bili su procenjeni na slici najvećeg poprečnog preseka prostate.

Correspondence to: Katarina Rajković, Laboratory for Image Analysis, Institute of Biophysics, Faculty of Medicine, University of Belgrade, 11 129 Belgrade, Serbia. Phone/Fax: +381 11 3607 068. E-mail: katar1970@yahoo.com

Rezultati. Ispitivani uzorak obuhvatio je četiri faze (TRUS prostate pre prve, druge, treće i četvrte HDR-BT frakcije). Statistička analiza pokazala je da u toku HDR-BT frakcije nije bilo značajne razlike u srednjoj vrednosti površine, kao ni u obliku kapsule prostate na njenom najvećem preseku. **Zaključak.** Kvantitativna analiza TRUS aksijalne segmetisane slike prostate pokazala je uspešno ocrtavanje prostate u seriji ručno segmentisanih TRUS slika i nepromenjen oblik prostate na najvećem njenom preseku u toku HDR-BT frakcija.

Ključne reči:
prostata, neoplazme; ultrasonografija; brahiterapija; modeli, teorijski.

Introduction

Prostate carcinoma is a common cancer and the second most common cause of cancer deaths in males [1]. Therapeutic management of prostate carcinoma has become complex, multidisciplinary and stage-specific [2, 3]. Treatment options for patients with localized, organ confined prostate carcinoma range from observation, radical prostatectomy, radiation therapy (external and/or brachytherapy), hormonal therapy and various combinations of these [3–5].

Prostate brachytherapy (BT) is one of definitive treatment options for low risk organ confined carcinoma [6–8] and intermediate-risk prostate carcinoma [9–14]. BT dose patterns and fractionation predominantly depend on BT modality [low-dose rate (LDR) or high-dose rate (HDR)] [15–17], disease stage, tumor/target volume, therapy scope (definitive/monotherapy, boost or salvage), status of the organs at risk (urethra and rectum) and patient performance status.

In practice, the final prostate contours for BT pre-planning or BT post-implantation planning could be obtained using manual, semi-automatic or automatic segmentation of the prostate margin images obtained by computed tomography (CT), magnetic resonance image (MRI) or transrectal ultrasound (TRUS) [18–23]. However, the prostate delineation, BT pre-planning and catheter implantation BT procedures are commonly based on the use of manually segmented TRUS images obtained in axial and sagittal plains [6, 15, 22] (Figure 1).

Precise information about the size and the shape of prostate plays a key role in BT implantation and planning processes. Manual TRUS prostate capsule segmentation (delineation) is known to be difficult and hardly reproducible due to interference of numerous unfavorable factors [24, 25]. Despite these downsides, TRUS in the prostate diagnostics value is not inferior to CT or MRI [24].

An important issue in prostate BT is the quality and consistency of prostate segmentation by TRUS. It is well-known that human expert performance (urologist and/or radiation oncologist/brachytherapist) in manual segmentation, measured as the prostate BT workload, can affect final therapy result [26], especially when fractionated high dose rate BT (HDR-BT) treatment planning is based on TRUS segmented prostate images.

However, when prostate HDR-BT is concerned, more than one implantation procedure could be applied. In these cases, it would be beneficial to have data on quantitative analysis of precision and consistency in prostate two dimensional (2D) TRUS axial image segmentation. Also, it would be beneficial to have precise information about the shape of the prostate during BT. Therefore the purpose of this study was to analyze consistency of the prostate capsule delineation prior to each HDR-BT fraction and the changes in the axial shape of the prostate capsule during HDR-BT using TRUS imaging.

Methods

Patients

A group of 16 patients, aged 65–82 years, in good health condition and performance status were treated at the Medical System Belgrade Brachytherapy Department, with definitive temporary HDR-BT (Microselectron HDR, ELECTA-Nucletron, the Netherlands). The total applied median dose was 52 Gy divided into four individual fractions, each fraction being delivered 2–3 weeks apart. The total HDR-BT dose was tailored individually, based on the selected association criteria of the American Brachytherapy Society [27]. The applied HDR-BT technique has been explained in detail elsewhere [4, 28]. Androgen blockade therapy was applied to the group of patients 2–3 months prior to HDR-BT in order to intensify prostate encapsulation and shrink prostate volume (not necessarily uncirculated).
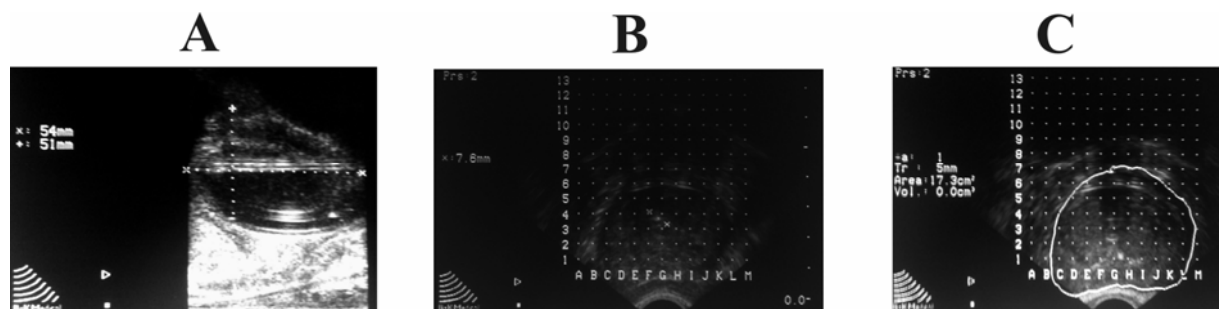

Fig. 1 – Typical transrectal ultrasound (TRUS) images of the prostate, shown with permission of the General Hospital Medical System Belgrade (MSB): A) sagittal plan, B) axial plan and C) segment axial plan at the maximum prostate cross-sectional area.

TRUS data acquisition

Patients were placed in lithotomy position under spinal anesthesia. Two parallel needles were positioned laterally to the prostatic urethra (Figure 1C) in order to prevent prostate movement during TRUS imaging and afterwards needle placement. Real time prostate axial visualization and manual segmentation prior each fraction was performed using B-K Medical Ultrasound (Model Hawk 2102) with a 7.5 MHz bi-plane TRUS probe mounted on a prostate-stepper. Manual segmentation, done by a single therapist, was performed from the prostate base (image b_0) to the prostate apex (b_a), using a $5 \cdot 10^{-3}$ m step (0 denotes a segment position from the prostate base and apex segment position). Prior to segmentation, Nucletron $5 \cdot 10^{-3}$ m grid was attached, centered and calibrated, allowing accurate rigid catheter/needle insertion. The median prostate volume calculated from TRUS data (V_{pc}) and volume (V_p) obtained by other means (CT or MRI), were $56 \cdot 10^{-6}$ m^3 (range 30–85·10^{-6} m^3), and 43 cm^3 (range 30–68·10^{-6} m^3), respectively, with the mean V_{pc}/V_p ratio of 1.4. The prostatic urethra volume was included in the calculated prostate volume.

For each patient, four imaging phases were completed and recorded: phase I – segmentation data collected before the first HDR-BT fraction; phase II – segmentation data collected before the second HDR-BT fraction; phase III – seg-mentation data collected before the third HDR-BT fraction; phase IV – segmentation data collected before the fourth HDR-BT fraction. A representative TRUS images prostate segment at the maximum axial cross sections (Figure 2) was used for HDR-BT pre-planning and catheter/needle application. The difference of maximum axial cross sections shown in Figure 2 can be directly related to the prostate volume changes between HDR-BT fractions. Post-therapy TRUS in the treated patients was not scheduled since this type of examination was not mandatory in HDR post-treatment evaluation protocol.

Image processing

All axial 2D-TRUS images were imported into the Image J, specialized public domain software for image analysis, developed by the National Institute of Health (USA, www.rsb.info.nih.gov/ij). Schematic representation of TRUS image processing procedure is illustrated in Figure 3. In the first step of the procedure grey-scale (Figure 3B) images were converted into the binary images (Figure 3A) using 'Threshold' tools. Figure 3B shows the silhouette area of the prostate capsule. In the second step of the procedure, binary images (Figure 3B) were converted into outline images (Figure 3B) using 'Outline' tools. Figure 3C shows the contour of the prostate capsule.
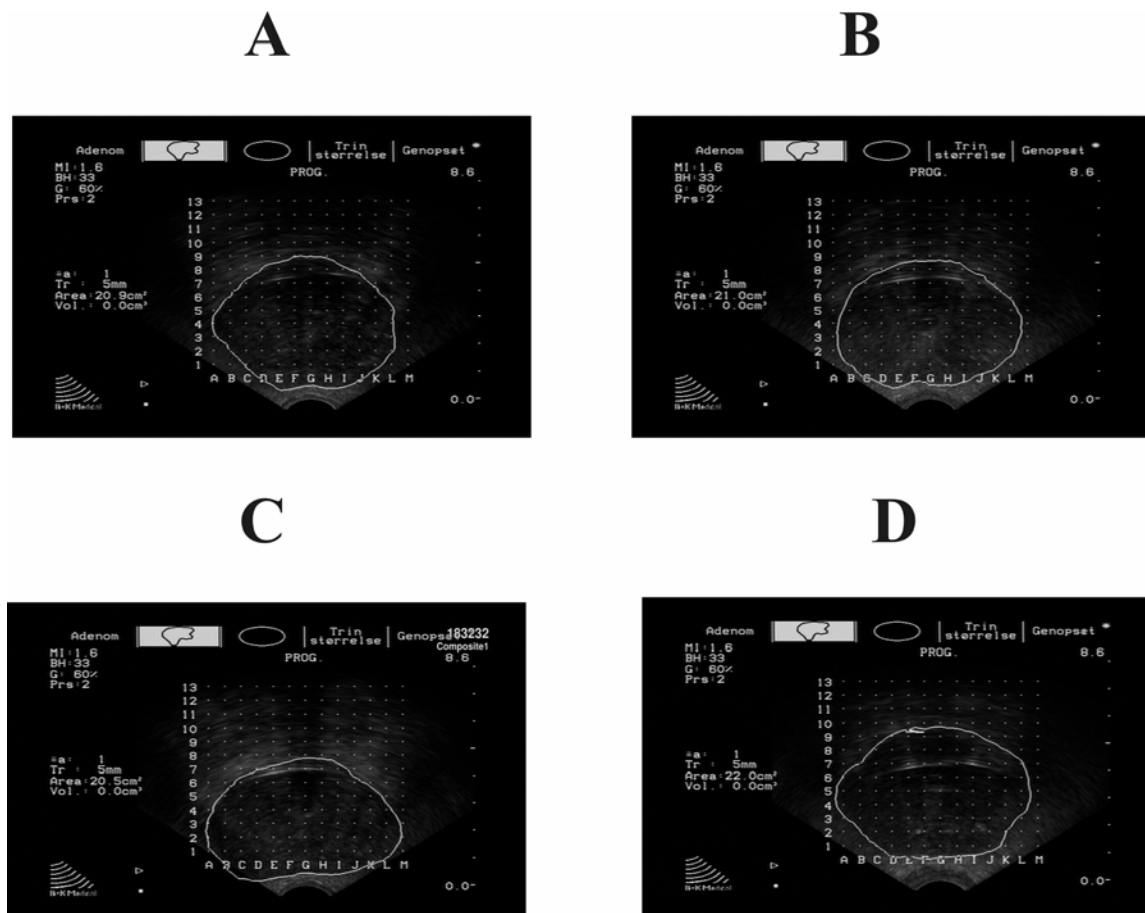

Fig. 2 – Representative two dimensional transrectal ultrasound (2D-TRUS) images of the prostate at the maximum axial cross section for the individual patient: A) phase I; B) phase II; C) phase III; D) phase IV.
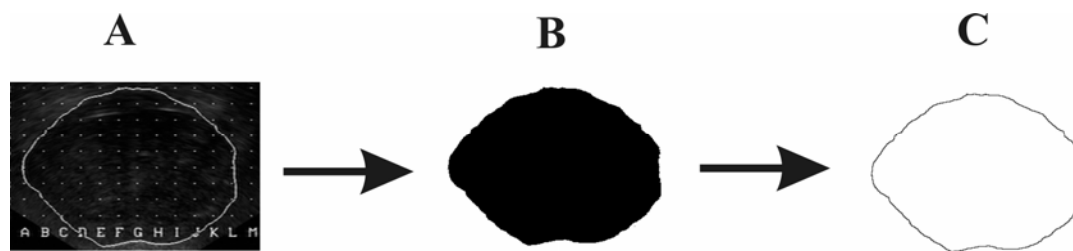
Fig. 3 – Schematic representation of the two-dimensional transrectal ultrasound (2D-TRUS) axial image of the prostate capsule processing procedure: grayscale image (A), image of the silhouette area (B) and of contour (C).

Quantitatively analyses of two dimensional TRUS axial image of the prostate capsule

Area analysis of the TRUS axial image of the prostate capsule

The cross sectional area of the prostate capsule (A) was measured on a particular 2D-TRUS axial image. The area measurement was carried out using TRUS standard calculation algorithm by B-K Medical Ultrasound (Model Hawk 2102). The average value of the cross-sectional area of the prostate (A_{av}) for segmentation data collected before the first, second, third and the fourth HDR-BT fraction (phase I; phase II; phase III; phase IV) was calculated (Figure 4).

Shape analysis of the TRUS axial image of the prostate capsule

Shape analysis of the prostate was estimated by two parameters: the fractal dimension and the circularity ratio of the prostate capsule contour. The parameters of the prostate shape were estimated at the maximum cross section. These parameters were obtained by using Image J.

Fractal dimension of the prostate capsule contour

The fractal dimension of the prostate contour at the maximum axial cross-section (D_{max}) defines the irregularity in the shape of the image, showing shape deviation from the corresponding circle ($D_{circle} = 1.254$) (Figure 5A). The image of the contour was analyzed by fractal analysis using the box-counting method [29, 30]. This method consists of "covering" the image outline with sets of squares (Figure 5B). Each set is characterized by the size r of the square edge. The corresponding number of squares N that is necessary to cover the image outline is presented as a function of r (Figure 5C). D_{max} is determined from the absolute slope value of the log–log relationship between $N(r)$ and r (Figure 5C). In performing box-counting method, the box sizes were scaled to the base of 2; that is, 2^1, 2^2... 2^k, where k continues until N is equal to unity [31]. Depending on the contour image size, the box-sizes were taken from 2 to 512 pixels.

Circularity of the contour prostate capsule

Although the prostate contours seem generally circular by nature, in practice we noticed a significant deviation of the prostate contours from the circle. A shape of the prostate capsule contour at the maximum axial cross section was estimated by using the circularity ratio (C_{max}). This parameter represents a measure of how particular shape deviates from a corresponding circle. If it is a circle contour, the circularity ratio is equal to one. In case of any other contour shape, the circularity ratio is less than one. This parameter is expressed as $C = 4\pi A P^{-2}$, where A is the area and P is the perimeter of the contour (Figure 6) [31].

Statistical analysis

Statistical analysis of the calculated prostate parameters depends on whether the distribution is normal or not. In the
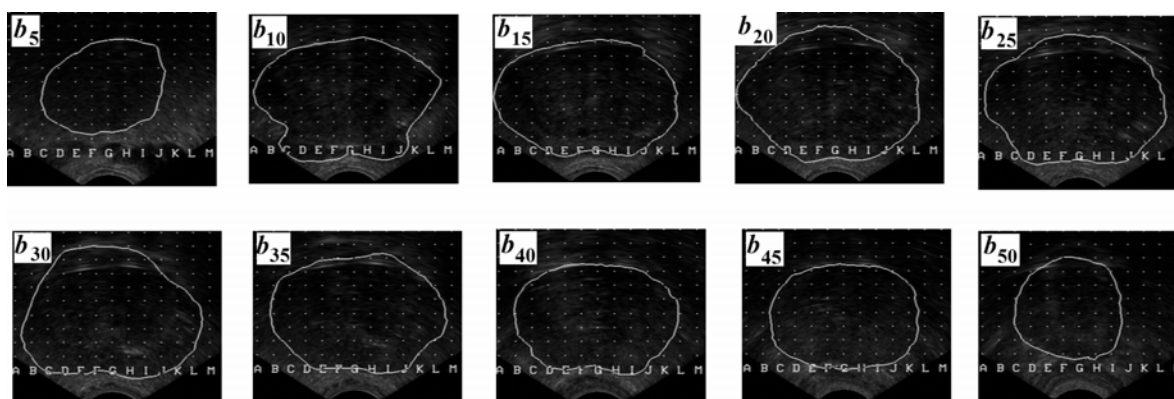

Fig. 4 – Two-dimensional transrectal ultrasound (2D-TRUS) axial images of prostate, from the prostate base (b_0) to the prostate apex (b_{50}). The cross-sectional area of the prostate capsule (A) from phase I brachytherapy in one patient; b_5 ($A = 9.9 \cdot 10^{-4}$ m^2), b_{10} ($A = 10.5 \cdot 10^{-4}$ m^2), b_{15} ($A = 19.8 \cdot 10^{-4}$ m^2), b_{20} ($A = 20.9 \cdot 10^{-4}$ m^2), b_{25} ($A = 20.1 \cdot 10^{-4}$ m^2), b_{30} ($A = 20.3 \cdot 10^{-4}$ m^2), b_{35} ($A = 18.3 \cdot 10^{-4}$ m^2), b_{40} ($A = 15.6 \cdot 10^{-4}$ m^2), b_{45} ($A = 14.5 \cdot 10^{-4}$ m^2), b_{50} ($A = 10.1 \cdot 10^{-4}$ m^2).
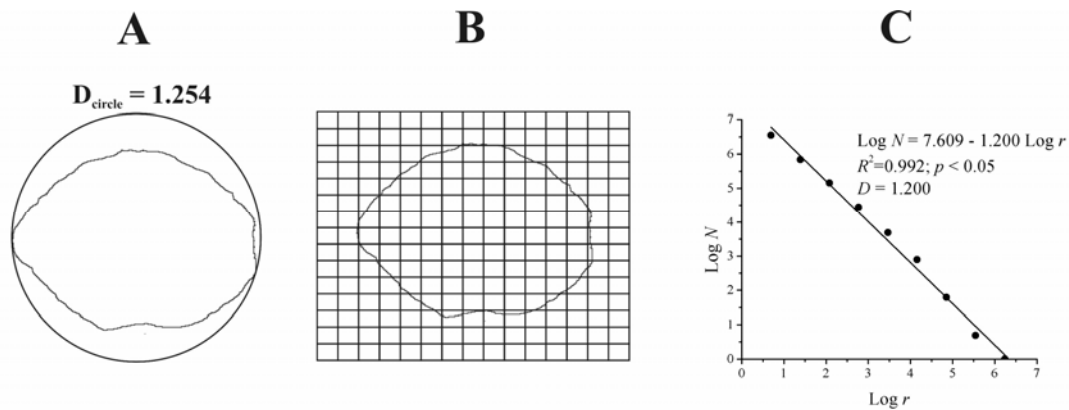
Fig. 5 – Illustration of calculating the fractal dimension of the prostate capsule contour, the fractal dimension of the circle is inscribed in the upper part of the figure (A). The application of the box-counting method to the contour, the whole image is covered with a set of squares and the squares which cover inner contour are counted (B). Log–log plot between the numbers of squares (N) and square size (r) is fitted by a straight line (C). The fractal dimension is 1.200, R^2 is the corresponding determination coefficient and p is the significance level.
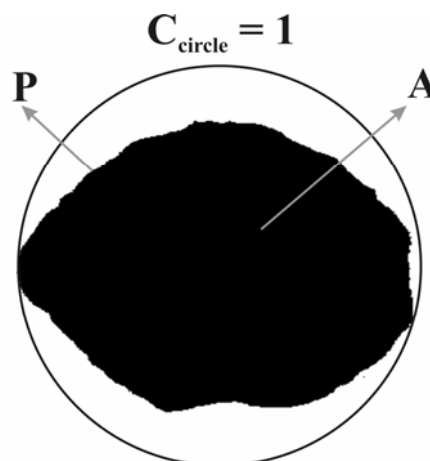

Fig. 6 – Illustration of circularity ratio calculation for the prostate capsule contour ($C = 4\pi AP^2$, A is the area and P is the perimeter). The circularity ratio of the circle is inscribed in the upper part of the figure.

case of calculated parameters showing a normal distribution, each group is described by the corresponding mean value and standard error [32]. If the number of patients is smaller than 30, the character of distribution has to be tested by calculation of two statistical parameters: skewness, a_3 and excess of distribution, e [33]. Briefly, the intervals of skewness and excess values, which define the normal distribution, are estimated when these two parameters are divided by the corresponding mean square errors (σ_3 and σ_4). If the absolute value of the quotients σ_3/a_3 and σ_4/e is less than or equal to 2, the data distribution can be considered as normal. Otherwise, the distribution of a sample (or population) has no characteristics of a normal distribution [34]. A statistical significance between mean values of parameters of prostate for 4-phase brachytherapy was estimated by Student´s t-test [34].

Results

The sample group consisted of four phases, each phase being performed prior to the first (phase I), second (phase II),

third (phase III) and the fourth (phase IV) BT fraction, respectively. Their representative axial images are shown in Figure 2. Table 1 shows value of the absolute ratios σ_3/a_3 and σ_4/e, for the average value of area (A_{av}), the fractal dimension (D_{max}) and the circularity ratio (C_{max}) for all four phases,. The absolute ratios (σ_3/a_3) and (σ_4/e) for the two parameters in all four of the phases are smaller than the critical value of 2. Therefore, the calculated values of three parameters showed normal distribution. Consequently, the values of three parameters of prostate capsule (A_{av}, D_{max} and C_{max}) can be expressed by the mean value and standards error.

The mean and standard errors of the A_{av}, D_{max} and C_{max} for four phases were presented in Table 2. It was noticed that all phases had similar mean values of the three parameters of the prostate capsule. The statistical test estimated the difference between the parameters of mean values for 4-phase brachytherapy.

In the next step, the mean values of all possible pairs were tested by t-test (Table 3). The t-values of all three parameters are less than the t-values tabulated at the level of

Values of σ_3/a_3 and σ_4/e for the average value of the area (A_{av}), the fractal dimension (D_{max}) and the circularity ratio (C_{max}) of the prostate capsule for 4-phase high-dose rate brachytherapy (HDR-BT)

Phase	Parameter of the prostate capsule					
	A_{av}		D_{max}		C_{max}	
	σ_3/a_3[e]	σ_4/e[f]	σ_3/a_3[e]	σ_4/e[f]	σ_3/a_3[e]	σ_4/e[f]
I[a]	0.28	0.78	0.13	0.22	0.27	0.67
II[b]	0.22	0.51	0.27	0.79	0.33	0.95
III[c]	0.28	0.89	0.13	0.22	0.14	0.22
IV[d]	0.30	1.07	0.33	0.99	1.72	0.92

[a]Segmentation data collected before the first HDR-BT fraction; [b]segmentation data collected before the second HDR-BT fraction; [c] segmentation data collected before the third HDR-BT fraction; [d]segmentation data collected before the fourth HDR-BT fraction; [e]mean square errors/skewness values; [f]mean square errors/excess values.

The average value* of the area (A_{av}), the fractal dimension (D_{max}), and the circularity (C_{max}) of the prostate capsule for 4-phases high-dose rate brachytherapy (HDR-BT).

Phase	$A_{av} \cdot 10^4$ (m^2)	D_{max}	C_{max}
I[a]	13 ± 3	1.19 ± 0.04	0.75 ± 0.07
II[b]	13 ± 2	1.19 ± 0.04	0.74 ± 0.06
III[c]	12 ± 3	1.19 ± 0.03	0.76 ± 0.03
IV[d]	13 ± 3	1.19 ± 0.04	0.75 ± 0.04

For abbreviations see under Table 1
*Each value is presented as the mean ± standard error.

The results of Student's t-test: t-values of the three parameters (A_{av}, D_{max} and C_{max}) of the prostate capsule given in Table 2 over pairs of the phases of high-dose rate brachytherapy (HDR-BT), tested for the significance

Pair of phases*	A_{av}	D_{max}	C_{max}
I[a]-II[b]	0.453	0.317	0.412
I[a]-III[c]	1.102	0.127	0.413
I[a]-IV[d]	0.605	0.102	0.437
II[b]-III[c]	0.766	0.226	1.060
II[b]-IV[d]	0.229	0.233	0.039
III[c]-IV[d]	0.456	0.021	1.389
$t_{0.05}$	2.131	2.131	2.131
$t_{0.01}$	2.947	2.947	2.947

For abbreviations see under Table 1

significance $p < 0.05$ and $p < 0.01$ (Table 3). The t-test showed that there were no statistical differences between all possible pairs of the means A_{av}, D_{max} and C_{max}, respectively (Table 3). Table 3 shows no significant difference in the values of A_{av}, D_{max} and C_{max}, for phase I, phase II, phase III and phase IV, respectively.

Discussion

TRUS is used to guide placement of implants during prostate BT [21], and as an input data for HDR-BT planning. This study quantitatively analyzed 2D-TRUS axial image obtained during prostate HDR-BT fractions. The average value area of cross section (A_{av}) and the two parameters relative to the maximum prostate capsule shape (D_{max} and C_{max}) were determined by analyzing 2D-TRUS axial image. Statistical analysis showed no significant differences in the average value of cross sectionsal area during, HDR-BT fractions (phase I, phase II, phase III and phase IV) as well as in the maximum shape of prostate capsule (D_{max} and C_{max}) (Table 3).

The absence of a significant difference in the average value of area (A_{av}) (Table 3) during prostate capsule delineation in the series of manually segmented TRUS images (phase I, phase II, phase III and phase IV) points to the consistency in prostate capsule delineation. This is in agreement with Solhjem et al. [19], who demonstrated a significant reproducibility in prostate volume measurement using TRUS. However, manual TRUS prostate capsule delineation is known to be hardly reproducible due to the interference of numerous unfavorable factors [24, 25]. This is the first time that the consistency in capsule delineation using TRUS was quantitatively proved, thus confirming a reproducibility of the manual TRUS segmented prostate axial images in pre-planning and catheter/needle application for the HDR-BT.

On the other hand, our results show that the maximum prostate shape (D_{max} and C_{max}) remains unchanged during analysis of HDR-BT fractions (Table 3). Holmes et al. [21] conducted shape analysis of the prostate, however, the fractal dimension and the circularity were used for the first time in our study to quantify the shape of the prostate capsule. The fractal dimension is a geometrical feature of irregularly shaped

objects [35]. Fractal analysis was applied to different medical images [36], but there is no data on its application to the 2D-TRUS axial images of the prostate. Also, it is analyzed by means of the circularity, now commonly used as a parameter which quantifies the shape of two-dimensional objects [31].

The lack of a significant difference in the shape of axial TRUS images during prostate capsule delineation in the series of manually segmented TRUS images (phase I, phase II, phase III and phase IV), could point to the absence of geometrical change in the fractions of HDR-BT. However, post HDR-BT data was not collected as TRUS in the treated patients. It was not mandatory in the HDR post-treatment evaluation protocol. Consequently, data for analysis of the prostate shape after the last treatment was not available.

The parameters of the cross-sectional prostate capsule (A_{av}, D_{max} and C_{max}) show that manually segmented TRUS images display good visibility necessary for precise delineation and monitoring of the prostate behavior during HDR-BT.

It was documented that prostate gland shrinkage may be expected in patients who undergo external beam radiotherapy shortly after starting androgen deprivation therapy [37]. Considering external beam radiotherapy alone, a particular effect of prostate gland shrinkage seems to be clinically insignificant [38].

Conclusion

In this study, the applied quantitative analysis of transrectal ultrasound axial prostate segmented images obtained in each phase shows a successful capsule delineation in the series of manually segmented transrectal ultrasound images done by a single therapist and that the prostate maximum axial shape remains unchanged during the high-dose rate brachytherapy course, of approximately 2-month duration.

This is the first time to determine the prostate capsule maximum shape (the fractal dimension and the circularity) of transrectal ultrasound axial images. These two prostate shape parameters may be applicable in quantification of prostate shape for the purpose of medical diagnostics and treatment. Transrectal ultrasound of the prostate is fast and relatively inexpensive diagnostic technique. Quantitative analysis showed that transrectal ultrasound of the prostate is accurate in pre-planning and catheter/needle application to high-dose rate brachytherapy. Additionally, the applied image analysis could be suitable for determination of the accuracy in other radiotherapy planning techniques.

R E F E R E N C E S

1. *Parkin DM, Pisani P, Ferlay J.* Global cancer statistics. CA Cancer J Clin 1999; 49(1): 33−64, 1.

2. *Acimovic M, Dabic-Stankovic K, Pejcic T, Dzamic Z, Rafailovic D, Hadzi-Djokic J.* Preoperative Gleason score, percent of positive prostate biopsies and PSA in predicting biochemical recurrence after radical prostatectomy. J BUON 2013; 18(4): 954−60.

3. *Heidenreich A, Bellmunt J, Bolla M, Joniau S, Mason M, Matveev V,* et al. EAU guidelines on prostate cancer. Part 1: screening, diagnosis, and treatment of clinically localised disease. Eur Urol 2011; 59(1): 61−71.

4. *Arsenijević T, Dabić-Stanković K, Aćimović M, Radošević-Jelić LJ.* Radiotherapy in Prostate Cancer.In: *Spiess* P, editor. Prostate Cancer: Diagnostic and Therapeutic Advances. Rijeka, Croatia: InTech; 2011.

5. *Mitsuzuka K, Koie T, Narita S, Kaiho Y, Yoneyama T, Tsuchiya N,* et al. Pathological and oncological outcomes of elderly men with clinically localized prostate cancer. Jpn J Clin Oncol 2013; 43(12): 1238−42.

6. *Blasko J, Radge H, Schumacher D.* Transperineal percutaneous iodine-125 implantation for prostatic carcinoma using tranrectal ultrasound and temlate guidance. Endocuriether Hypertherm Oncol 1987; 3: 131–9.

7. *Blasko JC, Wallner K, Grimm PD, Ragde H.* Prostate specific antigen based disease control following ultrasound guided 125iodine implantation for stage T1/T2 prostatic carcinoma. J Urol 1995; 154(3): 1096−9.

8. *Blasko JC, Grimm PD, Sylvester JE, Badiozamani KR, Hoak D, Cavanagh W.* Palladium-103 brachytherapy for prostate carcinoma. Int J Radiat Oncol Biol Phys 2000; 46(4): 839−50.

9. *Barkati M, Williams SG, Foroudi F, Tai KH, Chander S, van Dyk S,* et al. High-dose-rate brachytherapy as a monotherapy for favorable-risk prostate cancer: a Phase II trial. Int J Radiat Oncol Biol Phys 2012; 82(5): 1889−96.

10. *Demanes DJ, Martinez AA, Ghilezan M, Hill DR, Schour L, Brandt D,* et al. High-dose-rate monotherapy: safe and effective brachytherapy for patients with localized prostate cancer. Int J Radiat Oncol Biol Phys 2011; 81(5): 1286−92.

11. *Grills IS, Martinez AA, Hollander M, Huang R, Goldman K, Chen PY,* et al. High dose rate brachytherapy as prostate cancer monotherapy reduces toxicity compared to low dose rate palladium seeds. J Urol 2004; 171(3): 1098−104.

12. *Hoskin P, Rojas A, Lowe G, Bryant L, Ostler P, Hughes R,* et al. High-dose-rate brachytherapy alone for localized prostate cancer in patients at moderate or high risk of biochemical recurrence. Int J Radiat Oncol Biol Phys 2012; 82(4): 1376−84.

13. *Rogers CL, Alder SC, Rogers RL, Hopkins SA, Platt ML, Childs LC,* et al. High dose brachytherapy as monotherapy for intermediate risk prostate cancer. J Urol 2012; 187(1): 109−16.

14. *Yoshioka Y, Konishi K, Sumida I, Takahashi Y, Isohashi F, Ogata T,* et al. Monotherapeutic high-dose-rate brachytherapy for prostate cancer: five-year results of an extreme hypofractionation regimen with 54 Gy in nine fractions. Int J Radiat Oncol Biol Phys 2011; 80(2): 469−75.

15. *Das KR.* Prostate brachytherapy: HDR or seed implant. J Med Phys 2006; 31(4): 239−41.

16. *Cosset JM, Haie-Meder C.* Brachytherapy for prostate cancer: high dose rate or low-dose rate? Cancer Radiother 2005; 9(8): 610−9. (French)

17. *King CR.* LDR vs. HDR brachytherapy for localized prostate cancer: The view from radiobiological models. Brachytherapy 2002; 1(4): 219−26.

18. *Kälkner KM, Kubicek G, Nilsson J, Lundell M, Levitt S, Nilsson S,* et al. Prostate volume determination: Differential volume measurements comparing CT and TRUS. Radiother Oncol 2006; 81(2): 179−83.

19. *Solhjem MC, Davis BJ, Pisansky TM, Wilson TM, Mynderse LA, Herman MG,* et al. Prostate volume measurement by transrectal ultrasound and computed tomography before and after per-

manent prostate brachytherapy. Int J Radiat Oncol Biol Phys 2004; 60(3): 767−76.

20. *Buch K, Morancy T, Kaplan I, Qureshi MM, Hirsch AE, Rofsky NM,* et al. Improved dosimetry in prostate brachytherapy using high resolution contrast enhanced magnetic resonance imaging: a feasibility study. J Contemp Brachytherapy 2015; 6(4): 337−43.

21. *Holmes DR 3rd, Davis BJ, Goulet CC, Wilson TM, Mynderse LA, Furutani KM,* et al. Shape analysis of the prostate: establishing imaging specifications for the design of a transurethral imaging device for prostate brachytherapy guidance. Brachytherapy 2014; 13(5): 465−70.

22. *Litjens G, Toth R, van de Ven W, Hoeks C, Kerkstra S, Ginneken B,* et al. Evaluation of prostate segmentation algorithms for MRI: The PROMISE12 challenge. Med Image Anal 2014; 18(2): 359−73.

23. *Mahdavi SS, Chng N, Spadinger I, Morris WJ, Salcudean SE.* Semi-automatic segmentation for prostate interventions. Med Image Anal 2011; 15(2): 226−37.

24. *Pfengfei W, Yiguang L, Yongzhong L, Liping C.* TRUS Image segmentation driwen by narrow band contrast pattern using shape space embedded level sets. In: *Jian Y, Fang F, Changyin S,* editors. Intelligent Science and Intelligent Data Engineering: Lecture Notes in Computer Science. Berlin, Heidelberg: Springer-Verlag; 2013. p. 339−46.

25. *Pingkun Y, Sheng X, Baris T, Kruecker J.* Discrete deformable model guided by partial active shape model for TRUS image segmentation. IEEE T Biomed Eng 2010; 57(5): 1158−66.

26. Thompson S, Delaney G, Gabriel G, Izard MA, Hruby G, Jagavkar R, et al. Prostate brachytherapy in New South Wales: Patterns of care study and impact of caseload on treatment quality. J Contemp Brachytherapy 2015; 6(4): 344−9.

27. *Yamada Y, Rogers L, Demanes DJ, Morton G, Prestidge BR, Pouliot J,* et al. American Brachytherapy Society consensus guidelines for high-dose-rate prostate brachytherapy. Brachytherapy 2012; 11(1): 20−32.

28. *Skowronek J.* Low-dose-rate or high-dose-rate brachytherapy in treatment of prostate cancer - between options. J Contemp Brachytherapy 2013; 5(1): 33−41.

29. *Milosević NT, Ristanović D, Marić DL, Rajković K.* Morphology and cell classification of large neurons in the adult human dentate nucleus: A quantitative study. Neurosci Lett 2010; 468(1): 59−63.

30. *Ristanović D, Milosević NT, Stefanović BD, Marić DL, Rajković K.* Morphology and classification of large neurons in the adult human dentate nucleus: A qualitative and quantitative analysis of 2D images. Neurosci Res 2010; 67(1): 1−7.

31. *Milosević NT, Ristanović D, Jelinek HF, Rajković K.* Quantitative analysis of dendritic morphology of the α and δ retinal ganglion cells in the rat: A cell classification study. J Theor Biol 2009; 259(1): 142−50.

32. *Alder H, Roessler EB.* Introduction to Probability and Statistics. San Francisco, USA: WH Freeman and Co; 1972.

33. *Rajković K, Bačić G, Ristanović D, Milošević NT.* Mathematical Model of Neuronal Morphology: Prenatal Development of the Human Dentate Nucleus. Biomed Res Int 2014; 2014: 1−8.

34. *Riffenburgh RH.* Statistics in Medicine. London, UK: Academic Press; 1999.

35. *Di Ieva A, Grizzi F, Sherif C, Matula C, Tschabitscher M.* Angioarchitectural heterogeneity in human glioblastoma multiforme: A fractal-based histopathological assessment. Microvasc Res 2011; 81(2): 222−30.

36. *Lopes R, Betrouni N.* Fractal and multifractal analysis: A review. Med Image Anal 2009; 13(4): 634−49.

37. *Sanguineti G, Marcenaro M, Franzone P, Foppiano F, Vitale V.* Neoadjuvant androgen deprivation and prostate gland shrinkage during conformal radiotherapy. Radiother Oncol 2003; 66(2): 151−7.

38. *Budiharto T, Slagmolen P, Hermans J, Maes F, Verstraete J, Heuvel FV,* et al. A semi-automated 2D/3D marker-based registration algorithm modelling prostate shrinkage during radiotherapy for prostate cancer. Radiother Oncol 2009; 90(3): 331−6.